Forest Ecology and Management 529 (2023) 120652

Contents lists available at ScienceDirect

Forest Ecology and Management

journal homepage: www.elsevier.com/locate/foreco

Understanding and modelling the dynamics of data point clouds of relative growth rate and plant size

Arne Pommerening [a,*], Guillermo Trincado [b,c], Christian Salas-Eljatib [d,e,f], Harold Burkhart [g,1]

[a] Swedish University of Agricultural Sciences SLU, Faculty of Forest Sciences, Department of Forest Ecology and Management, Skogsmarksgränd 17, SE-901 83 Umeå, Sweden
[b] Instituto de Bosques y Sociedad, Facultad de Ciencias Forestales y Recursos Naturales, Universidad Austral de Chile, Valdivia, Chile
[c] Modelo Nacional de Simulación (MNS), Facultad de Ciencias Forestales, Universidad de Concepción, Concepción, Chile
[d] Centro de Modelación y Monitoreo de Ecosistemas, Facultad de Ciencias, Universidad Mayor, Santiago, Chile
[e] Vicerrectoría de Investigación y Postgrado, Universidad de La Frontera, Temuco, Chile
[f] Departamento de Silvicultura y Conservación de la Naturaleza, Universidad de Chile, Santiago, Chile
[g] Department of Forest Resources and Environmental Conservation, Virginia Polytechnic Institute and State University, Blacksburg, VA, USA

ARTICLE INFO

Keywords:
Plant development and life-history traits
Ontogenetic drift
Elliptic data clouds
Spatially-explicit model
Growth analysis
Growth dominance

ABSTRACT

Relative growth rates (RGR) have both intrigued and irritated many plant scientists since they were proposed as characteristics of growth performance in the early 20th century. Particularly, the common trend of RGR to decrease with increasing size, also referred to as *ontogenetic drift*, has given rise to many debates and much criticism. In this study, we showed that, with plants that germinated at the same time, it is common to obtain a linear relationship between RGR and size for each survey year which – when pulled together in one graph – eventually form a system of cascading elliptical point clouds over time. This system of data point clouds reflects the well-known exponential decline of RGR with size, the aforementioned ontogenetic drift. Using 12 individual-tree time series of *Pinus radiata* in Chile we studied the ontogenetic drift based on a new spatially explicit explanatory model allowing the reconstruction of individual-tree RGR trajectories. Favourable environmental conditions enforced the RGR decline over size and accelerated growth dynamics. Less favourable environmental conditions reduced the strength of the ontogenetic drift and slowed down growth. We also found that the model parameter estimates were more precise the stronger the RGR decline over size. Both, interpretable model parameters and evaluation characteristics, described the ontogenetic drift well. Interestingly, the slopes of the semi-major axes of the RGR-size data ellipses changed signs precisely at the time when smaller trees ceased to dominate population growth and larger trees started to contribute disproportionately to the overall growth processes.

1. Introduction

Relative growth rate (RGR) is a measure widely considered in various fields of plant science including plant physiology, plant ecology and plant growth. RGR is an important indicator of life performance of organisms and therefore closely related to plant physiology and plant mortality (Houghton et al., 2013; Bigler and Bugmann, 2003). It is a pre-requisite for quantifying and modelling allometric relationships in plants (Niklas, 1994). A crucial benefit of studying relative plant growth is the avoidance, as far as possible, of the inherent differences in scale between contrasting organisms so that their performances may be compared on an equitable basis (Hunt, 1990). Wenk et al. (1990) stated that relative growth rate is an expression of "growth energy" and Causton (1977) asserted that RGR is a measure of the efficiency of plant material to produce new organic material, i.e. net primary production (NPP) as a proportion of plant biomass, and that it is therefore a crucial physiological characteristic. In more recent work, efficiency is often defined as the ratio of net primary production (NPP) and gross primary production (GPP) (Rose et al., 2009; Rees et al., 2010). RGR has also become an important characteristic for separating species into functional groups according to their growth strategy (Houghton et al., 2013; Grime, 1977).

* Corresponding author.
E-mail address: arne.pommerening@slu.se (A. Pommerening).
[1] Deceased on 20 October 2022.

https://doi.org/10.1016/j.foreco.2022.120652
Received 15 August 2022; Received in revised form 4 November 2022; Accepted 13 November 2022
Available online 25 November 2022

Relative growth rate is primarily a function of time and is defined as the increase in size relative to the size characteristic itself. As instantaneous growth rates cannot be measured in the field, the difference between size characteristics of interest is usually studied at discrete points in time, k, which, for example, are scheduled survey years (Pommerening and Muszta, 2016). According to Blackman (1919), Fisher (1921), Whitehead and Myerscough (1962) and Hunt (1982, 1990), mean periodic relative growth rate, $\bar{p}_k$, is the difference of the logarithms of y_k and y_{k-1} divided by the difference in time, see also Causton (1977, p. 213):

$$\bar{p}_k = \frac{\log_e y_k - \log_e y_{k-1}}{t_k - t_{k-1}} \quad (1)$$

where $k = 2, \cdots, n$ denote scheduled survey years, t is time in years and y is an arbitrary size characteristic, e.g. tree stem diameter. Blackman (1919) originally referred to Eq. (1) as "efficiency index" and "specific growth rate" and the characteristic is thought to reflect systematic variation in physiology, allocation and leaf construction (Houghton et al., 2013). Mean periodic relative growth rate is in fact the most common RGR measure used in plant sciences and as such the characteristic reflects intrinsic growth physiology when comparing plant growth potential (Turnbull et al., 2008). In the remainder of the text, for ease of reading we will use RGR and $\bar{p}_k$ (p) as synonyms, but note there are different characteristics of RGR (see Pommerening and Grabarnik, 2019, Chap. 6) and the abbreviation sometimes refers to discrete measures (e.g. in Eq. (1), $\bar{p}_k$) and sometimes to functions (e.g. in Eq. (2), p).

In a negative exponential fashion, RGR continuously decreases with increasing time and size, a trend sometimes referred to as *ontogenetic drift* (Evans, 1972). The ontogenetic drift is consistent with the explanatory model involving the concept of growth dominance proposed by Binkley et al. (2006), which is supported by recent thinking on changes in physiological processes with tree size. The ontogenetic drift has been attributed to a decline in photosynthetic production in consequence of increased water stress in leaves of larger trees as described by the *hydraulic limitation hypothesis* (Ryan and Yoder, 1997; Ryan et al., 2006). Other studies (Yoda et al., 1965; Binkley, 2021; Rees et al. 2010; see West, 2020 for an overview) have suggested the phenomenon is a consequence of increased respiratory losses (*respiration hypothesis*), as taller trees incur greater metabolic costs. These physiological effects interact with tree competition and together determine the changes of RGR in relation to tree size.

Since age information is not always available and for obtaining a clearer understanding of growth trends, RGR has increasingly been related to plant size (Rose et al., 2009; Rees et al., 2010). In experiments in general plant science and in tree plantations, where commonly all individuals are of the same age and species, the relationship between RGR and plant size in a given survey year often appears to be linear and the data points are arranged in elliptic point clouds (Fig. 1). This has given rise to several linear models, see, for example, Iida et al. (2014) and Dyer (1997). However, the RGR-size point-cloud shape can vary considerably between data sets (Larocque and Marshall, 1993): According to Perry (1985), Larocque and Marshall (1993), a *decline in RGR* with increasing tree size (phase 1, e.g. point cloud of 1994 in Fig. 1) indicates that competition does not exist or is not severe enough to induce mortality. This period corresponds to a phase in which the efficiency of trees to produce new biomass is inversely related to their size: the smaller the tree, the more efficient it is at producing new biomass. Although dominant trees with large crowns have the highest photosynthetic production, they would be less efficient because of greater maintenance respiration needs resulting from larger roots, stems and branches. When *RGR remains constant* with tree size (phase 2, e.g. point cloud of 1995 in Fig. 1), it indicates that competition is beginning to become important enough to induce mortality. Finally, an *increase in RGR* with an increase in tree size (phase 3, e.g. point clouds of 1996 and 1997 in Fig. 1) indicates severe competition: suppressed trees become

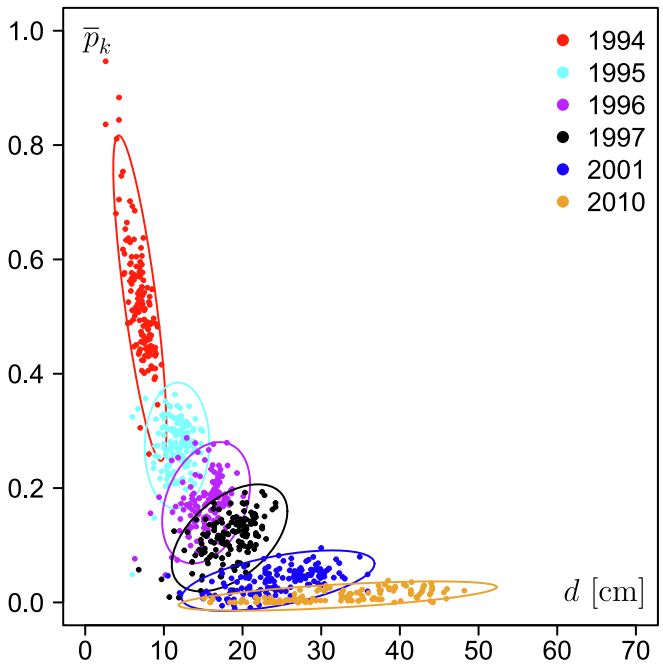

Fig. 1. Temporal progression of the RGR ($\bar{p}_k$)-d point clouds in even-aged *P. radiata* plot 410211 (see Section 2.8). The colours refer to different discrete census years reflecting different tree development stages and are highlighted by 95%-confidence ellipses. d is individual-tree stem diameter. (For interpretation of the references to colour in this figure, the reader is referred to the web version of this article.)

less efficient at producing biomass than larger trees. This interpretation is consistent with the growth dominance model proposed by Binkley et al. (2006).

In natural forests, however, RGR values mostly follow a declining exponential trend in each survey year with small trees having large RGR values and large trees showing small RGR values (Pommerening and Grabarnik, 2019). The same pattern is confirmed for the RGR development of individual trees with time, for example, when carrying out stem analyses or when considering the growth rates of individual trees measured in repeated forest inventories (Bragg, 2001; Pommerening and Grabarnik 2019, Chap. 6). In even-aged tree plantations and in greenhouse/field experiments involving other plants, the RGR-size point-clouds often have elliptic shapes thus suggesting linear relationships (Ramseier and Weiner, 2006). This first impression of data ellipses may continue to persist, but when data from more than one survey of the same population are available, it can be shown that pulling all RGR-size point clouds together and arranging them in one graph gives the same declining or negative exponential trend observed in natural ecosystems (Pommerening and Grabarnik, 2019, Fig. 1). At the beginning of such time series, i.e. at a stage of early size development, the point clouds are almost vertical with only a small tilt to the right or left, i.e. RGR declines with increasing tree size (Fig. 1, phase 1). With progressing plant development and increasing plant size the tilt increases and there is some overlap between point clouds (phase 2). The aforementioned trend is progressively lost and RGR tends to bear little or no relation to tree size. By the final two survey periods there is a clear tendency for RGR to increase with increasing size (phase 3).

The tilting and the shape of the data ellipses is partly a consequence of increasing size variance and decreasing RGR variance in subsequent surveys. These two simultaneous effects initially increase but then gradually decrease the strength of the linear relationship (Pommerening and Grabarnik, 2019). This can be thought of as being caused by individual trees with larger RGR values moving faster on declining trajectories of relative growth than trees with small initial RGR values. As a

consequence, trees with larger RGR values tend to develop larger tree sizes faster. However, tilting and shape of the data ellipses are also a consequence of the effects of size on growth.

The objective of this paper is to better understand and to model the dynamics of RGR and their dependence on plant size. To achieve this goal we developed a simple, spatially explicit model explaining and simulating the development of elliptic RGR-size relationships. This new dynamic model sheds light into the gradual ontogenesis of relative growth rate – size point clouds. The modelling approach is generic and can be applied to data from any plant field or laboratory trial. In this study, we used tree data as application data.

2. Materials and methods

2.1. Spatially explicit RGR modelling concept

We modelled relative growth rates (RGR) based on an extension of the Gompertz function (Gompertz, 1825) following Wenk (1969) and Wenk et al. (1990, p. 80). This modified Gompertz function is:

$$p = e^{-c_1 \times d \times \left(1-e^{-c_2 \times S}\right)} \text{ with } d, S > 0 \quad (2)$$

where p is RGR, d is tree stem diameter (cm) representing tree size and S is the spatially explicit *hyperbolic tangent index* expressing plant dominance and exposure to competition (Pommerening et al., 2020). S is unlikely to take the value of 0. Theoretically d and S can be replaced by other suitable plant characteristics describing size and interaction. Even non-spatial measures of plant interaction can be considered. The hyperbolic tangent index is convenient because its values always lie within a range of 0 and 1. It has also proved to explain growth rates well (Pommerening et al., 2020). Using d as size characteristic the variant of the hyperbolic tangent index S used in our study is defined for ~~tree~~ subject tree i as

$$S_i = \frac{1}{\sum w_j} \sum_{j=1}^{n} \frac{d_i^{2\alpha}}{d_i^{2\alpha} + d_j^{2\alpha}} \times w_j \quad (3)$$

The number of nearest neighbours is denoted by n and parameter α accounts for symmetric ($\alpha = 0$) or asymmetric ($\alpha \to \infty$) competition (Freckleton and Watkinson, 2001). Symmetric competition is regarded as an equal sharing of resources amongst individuals, whilst asymmetric competition describes an unequal sharing, where large trees have a disproportionate advantage in competition with smaller trees (Weiner et al., 2001). The subject tree for which S is calculated is denoted by i and the nearest neighbours by j. The index values lie between 0 and 1 and the larger the index value the more dominant is the tree at hand. In addition, we defined a weight w_j as

$$w_j = \frac{g_j}{dist_j^{\delta}} \quad (4)$$

where $g_j = \pi(d_j/2)^2$ and $dist_j$ is the Euclidean distance between subject tree i and a neighbour tree j. This weight (Eq. (4)) models the decay of size dominance with increasing distance and therefore puts greater emphasis on close neighbours and on neighbours of large size. (The same weight can also be employed when size variables other than d were selected and biomass or volume would be alternatives.) The larger δ the stronger the focus on neighbouring trees in close proximity to subject tree i. We selected $n = 30$ neighbours to deliberately include a large number of nearest neighbours in order not to miss any important competitor and used periodic boundary conditions in all calculations (Illian et al., 2008, p. 184) to take edge effects into consideration.

The RGR function (Eq. (2)) was designed in such a way as to explain RGR (p) mainly in terms of plant size, in our case tree stem diameter d. Size dominance and competition, as represented by S, are only secondary considerations in Eq. (2), which particularly affect trees when they are medium-sized (Wenk et al., 1990). RGR of larger trees is then increasingly influenced by plant size alone (see Fig. 2A), i.e. with increasing size the influence of competition fades out which is very realistic.

By design, model parameter c_1 in Eq. (2), also referred to as the *growth parameter*, always has a stronger effect on RGR than parameter c_2 (Eq. (2)). Only small values of c_2 move the curve of the RGR function upwards. The growth parameter is negatively correlated with RGR and for individual trees lower values of c_1 imply increased growth. Smaller, more suppressed trees have lower RGR and accordingly higher c_1 values (Murphy and Pommerening, 2010). RGR increases with increasing values of size dominance S. For very low values of S, tree size does not matter much, but with increasing development, size influences the S-p relationship much more (Fig. 2B). Small trees benefit markedly more from increasing S than comparatively large trees.

Unlike in other modelling approaches, in our study each tree of a given tree population has a specific set of parameters c_1 and c_2. More

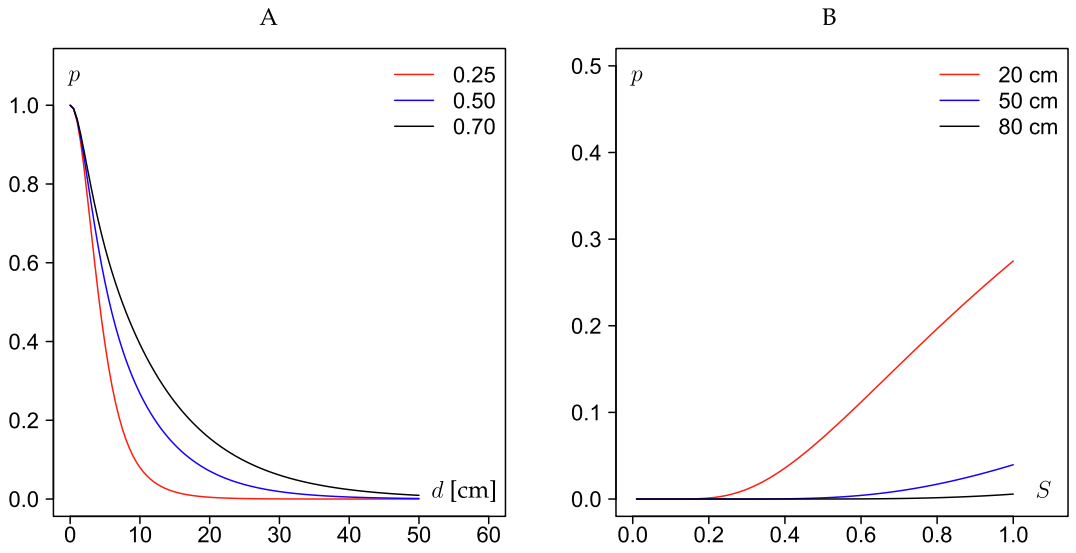

Fig. 2. RGR (p) function (Eq. (2)) for plot 205107 (see Section 2.8) and three different values of the hyperbolic tangent index S (0.25, 0.50, 0.70) with parameters c_1 and c_2 estimated through Eqs. (5) and (6) depicted over size (represented by stem diameter d, A) and spatial dominance (represented by the hyperbolic tangent index S (Eq. (3)), B) for three different values of d (20, 50, 80 cm). (For interpretation of the references to colour in this figure, the reader is referred to the web version of this article.)

importantly, these two parameters can change from simulation year to simulation year to better adapt to changing environmental conditions. This allows a tree to flexibly change the specific trajectory, according to which its RGR decreases, from simulation year to simulation year (Fig. 2A). We therefore replaced population parameters c_1 and c_2 in Eq. (2) by the two corresponding individual-tree parameters $c_{i,t}^{(1)}$ and $c_{i,t}^{(2)}$ using tree and time indices in the notation. In each simulation year, the two parameters are estimated based on the current values of d and S using Eqs. (5) and (6):

$$c_{i,t}^{(1)} = a_0 \times {S_{i,t}}^{-a_1} \tag{5}$$

$$c_{i,t}^{(2)} = b_0 \times {d_{i,t}}^{-b_1} \tag{6}$$

This approach of estimating the parameters of the growth function is reminiscent of the *parameter-prediction method* described in growth modelling textbooks (Clutter et al., 1983; Weiskittel et al., 2011; Burkhart and Tomé, 2012), but to our knowledge has not been applied to growth functions so far. The main purpose of Eqs. (5) and (6) is to achieve an individualisation of the function defined in Eq. (2) and the corresponding model parameters and thus greater flexibility. Individual-tree growth curves are now allowed to deviate from the common population trend of Eq. (2) and to follow observed individual-tree RGR trajectories. Both parameters $c_{i,t}^{(1)}$ and $c_{i,t}^{(2)}$ were found to correlate with both d and S and therefore, the decision was made to alternate the use of these two independent variables in Eqs. (5) and (6) compared to their role in Eq. (2). Once RGR (p_t) has been estimated using Eq. (2), stem-diameter growth is updated in the simulation for the next growth period based on Eq. (7):

$$d_{i,t+\Delta t} = d_{i,t} \times e^{p_t} \tag{7}$$

We modelled tree annual mortality rate, m, as a function of the reciprocal of tree size and of RGR of the previous growth period, $\bar{p}_{i,t-\Delta t}$, and we again applied the Gompertz function due to its statistical advantages (Gompertz, 1825; Salas-Eljatib and Weiskittel, 2020). The functional form of mortality rate $m_{i,t}$ is:

$$m_{i,t} = 1 - e^{-e^{m_0 \; + \; m_1 \; \times \; \frac{1}{d_{i,t}} \; + \; m_2 \; \times \; \bar{p}_{i,t-\Delta t}}} \tag{8}$$

where m_0, m_1 and m_2 are model parameters. Birth and ingrowth models were not considered here, as they hardly occur in general plant field trials, laboratory trials or in forest plantations.

2.2. Parameter estimation

Based on time-series data from observational plots the a/symmetry parameter α (Eq. (3)) and the distance exponent δ (Eq. (4)) were initially estimated through a grid search. That combination of α and δ was supposed to be selected that maximised the correlation between S and RGR. However, in most cases the grid-search results either led to situations where the range of S was extremely limited or to inferior simulation results with regard to the end diameter density distribution and the slope characteristic described in Section 2.6. Therefore, we decided to use the default values of $\alpha = 1$ and $\delta = 2$ for all 12 time series. These defaults have proved useful in other studies (Boyden et al., 2005; Pommerening et al., 2020): $\alpha = 1$ represents moderate asymmetric competition whilst $\delta = 2$ is often preferred in (Gaussian) competition kernel functions for its plausible behaviour including a focus on very close neighbours.

Parameters a_0, a_1, b_0 and b_1 (Eqs. (5) and (6)) were estimated simultaneously through least-squares regression. In addition, we estimated parameters c_1 and c_2 of Eq. (2) to quantify the mean growth trend of the entire tree population, however, these two parameters were not used in the model simulations. The mortality parameters were estimated separately using a Gompit regression model based on Eq. (8) that was fitted in a generalised linear modelling framework (Salas-Eljatib and Weiskittel, 2020).

2.3. Model scheduling

The model operates in discrete, annual time steps and at the beginning of each simulation year, first the mortality rule is applied followed by the removal of all dead trees. Afterwards the hyperbolic tangent index S is calculated. Current stem diameter and hyperbolic tangent index are used to estimate parameters $c_{i,t}^{(1)}$ and $c_{i,t}^{(2)}$ and thus contribute to the simulated annual relative growth rate based on Eq. (2). After calculating RGR, all stem diameters are updated synchronously using Eq. (7) to result in the stem diameters for the following year. A memory function saving previous RGR values is updated as the last step in each simulation year.

2.4. Stochasticity

A Gaussian random number with a mean of 0 and a standard deviation given by the standard error of residuals was added to the results of Eqs. (2). The mortality rule (Eq. (8)) was applied in such a way that the predicted mortality rate $m_{i,t}$ was compared with a uniform random number on the interval 0–1. Tree i is considered to have died, if $m_{i,t}$ is larger than the random number.

2.5. Model initialisation and simulations

The model was initialised with the tree list including all trees alive of the first year of the time series considered. For the application of the global envelope test (Myllymäki and Mrkvička, 2019), 4499 simulations were carried out independently for each of the 12 plots.

2.6. Model evaluation

For evaluating the regression results relating to the growth processes we quantified standard error of residuals, bias and RMSE. These characteristics always related to stem-diameter RGR. In addition, and for better comparison between data sets, we calculated *relative bias* and *efficiency* and these two characteristics also related to the growth processes only. Relative bias, B, is defined as

$$B = \frac{\sum_{i=1}^{n} (\hat{y}_i - y_i)}{n\bar{y}}, \tag{9}$$

where $\hat{y}_i$ is the ith prediction (modelled stem-diameter RGR), y_i is the ith observation (observed stem-diameter RGR), n is the number of observations and $\bar{y}$ is the mean observation. Efficiency, E, is defined as

$$E = 1 - \frac{\sum_{i=1}^{n} (\hat{y}_i - y_i)^2}{\sum_{i=1}^{n} (y_i - \bar{y})^2}. \tag{10}$$

Efficiency values approach one with improving model performance. A value of zero indicates that the model explains no more variation than the mean value of the observations alone and negative values highlight biased estimates.

In addition to these evaluation characteristics we also compared the stem-diameter density distribution of the last survey year with the envelopes obtained from 4499 simulations using the global envelope test (Myllymäki et al., 2018). Following the approach suggested by Dyer (1997), we also approximated the semi-major axes of the RGR-$d/\bar{d}$ data ellipses based on the slope parameter of this linear relationship using robust regression to minimise the influence of outliers. Here size was expressed as individual-tree stem diameter, d, relative to the mean stem diameter, $\bar{d}$, of the tree population in a given survey or simulation year. This slope characteristic is particularly important to judge whether the sequence of data ellipses (Fig. 1) was modelled correctly. These two additional evaluation characteristics reflected the performance of the entire model. Additionally, we compared the observed slope values with

the growth dominance coefficient. Growth dominance characterises the contributions of different tree sizes to total population growth (Binkley et al., 2006; West, 2014). The characteristic puts plant size and growth into a population-level representation by ranking plants from the smallest to the largest and plotting cumulative plant size over the corresponding cumulative growth. This results in a graph similar to the Lorenz curve (Lorenz, 1905). In contrast to the Lorenz curve, the growth dominance statistic considers tree sizes and tree growth rates at the same time. The growth dominance curve can be summarised in a single number, the growth dominance statistic or growth dominance coefficient G, which can also take negative values, particularly in the interesting case of forests with high tree size diversity. This number is the proportional area enclosed by the growth dominance curve. Negative G indicate situations where the growth of the largest plants is less than their proportional contribution to cumulative population size. Positive G highlight a situation where the growth of the largest plants is greater than their contribution to cumulative population size. Values of $G = 0$ imply that the growth of each plant is proportional to its contribution to cumulative population size.

For this analysis we used our own R (R Development Core Team, 2021) and C^{++} code additionally applied the GET package (Myllymäki and Mrkvička, 2019).

2.7. Mapping the parameter space

We wanted to understand how the individual model parameters of RGR growth processes related to the general population trend. To this end we plotted all individual-tree $c_{i,t}^{(1)}$ and $c_{i,t}^{(2)}$ parameters against each other in such a way that for each plot separately they were both standardised between 0 and 1 using the common min–max normalisation method. We also standardised the population parameters c_1 and c_2 in the same procedure. Finally, we subtracted standardised parameters c_1 and c_2 from the corresponding individual-tree $c_{i,t}^{(1)}$ and $c_{i,t}^{(2)}$ parameters so that population parameters c_1 and c_2 were located at (0, 0), i.e. the origin of the system of coordinates.

2.8. Study data

In principle, any plant data could be used for this study and stem diameter could be replaced by biomass, stem volume or weight. We used tree data as an example and deliberately selected observations from plantations to make the data more similar to data from general plant trials.

Spatio-temporal data for Monterey pine (*Pinus radiata* D. Don) trees growing in Chile were obtained from a network of silvicultural trials established between 1992 and 1996 by Modelo Nacional de Simulación (MNS). These trials were located in highly productive forest stands at the age of 5-years, originally with the purpose to evaluate the main and interactive effects of thinning, pruning and fertilization on tree- and stand-growth. Each trial was established as a randomized block design with three replicates. The average plot size was 1600 m^2 ranging from 1594 to 1676 m^2 and the average planting spacing was 3.0 m between rows and 2.5 m within row. From this network, two trials located on contrasting sites were selected for testing the proposed modelling approach. To make the study data more comparable to data from general plant trials, we selected two unthinned and unpruned plots from each block that were established without fertilization. Thus, for each trial, six plots were available for this study. Trial 205 is located in the Coastal Range (35°14′ S, 72°12′ W) on granite soils at 460 m a.s.l. with a mean annual temperature of 12.1 °C and a mean annual precipitation of 688.4 mm. The measured site index was 33.3 m at base age 20 years. By contrast, trial 410 is located in the Andean Piedmont (36°30′ S, 71°39′ W) on volcanic ash soils at 460 m a.s.l. with a mean annual temperature of 13.5 °C and a mean annual precipitation of 1207.4 mm. The measured site index was 36.3 m (at base age 20 years) showing higher productivity and carrying capacity in comparison to trial 205. Both trials were established in 1994 and were re-measured annually over a period of 14 (trial 205) and 16 years (trial 410). However, in both trials remeasurements were not performed in 2005 and 2009.

3. Results

3.1. RGR trajectories

The observed trajectories of relative growth rates markedly differed between the two trials 205 and 410. The trajectories of trial 205 are much flatter than those of the more productive trial 410 which have much more curved trajectories, i.e. a greater ontogenetic drift (Fig. 3).

In both trials there were occasional deviations of individual-tree trajectories from the population trend. These deviations occurred in all plots, however, they were greatest in plots 205211, 410107 and 410211. In some plots, this variability of RGR trajectories was particularly large in early years, e.g. in plots 205107, 410111, 410211 and 410307.

It is also evident that mortality trees, i.e. trees that do not survive the whole duration of the experiments, occupied the lower ranks of RGR trajectories particularly in survey years nearer to the time of their deaths. This is good confirmation of our mortality model (Eq. (8)), which included RGR of the previous growth period as independent variable. Some mortality trees had fairly high RGR values in early years of the experiments, but these values subsequently decreased more than those of other trees.

3.2. Model performance

The c_1 parameter of the general population trend is fairly homogeneous across trials. Arithmetic mean c_1 of trial 205 (Table 1) was 0.13 whilst the corresponding mean on trial 410 (Table 2) was 0.17. As parameter c_1 is an interpretable growth parameter, this difference reflects a difference in productivity (Murphy and Pommerening, 2010) which is higher in trial 410. As mentioned in Section 2.8, this trial showed a higher yield level (measured as site index) compared to trial 205. The higher productivity is a function of better environmental conditions for this species. Parameter c_2 is more related to tree dominance and there was no interpretable trend here, the values markedly varied from plot to plot.

It is interesting to note that in trial 410 all model parameters b_1 were negative, i.e. parameter $c_{i,t}^{(2)}$ increases with increasing stem diameter (Table 2) whilst in trial 205 in the majority of plots parameter b_1 was positive (except for plot 205107; Table 1). Positive b_1 implies that parameter $c_{i,t}^{(2)}$ decreases with increasing stem diameter. Plot 205107 had the strongest ontogenetic drift in trial 205 which may explain why parameter b_1 was negative here like for all plots in trial 410.

Mortality rates were generally very low in all 12 plots and the general pattern of mortality parameter values is consistent with no anomalies. The Gompertz mortality model (Eq. (8)) has proved to be a robust and reliable model.

The efficiency of all 12 models was generally remarkably high and ranged between 0.73 in plot 205211 and 0.95 in plot 410211. Incidentally, fitting models based on population parameters c_1 and c_2 instead of using Eqs. (5) and (6) in all 12 cases led to markedly lower efficiency values (not reported here) compared to those listed in Tables 1 and 2. Efficiency values were higher the stronger the ontogenetic drift and the more homogeneous the RGR trajectories (Tables 1 and 2). Overall, the performance results suggest that the chosen model is generally suitable for describing RGR individual trajectories adequately and offers the benefit of interpretable model parameters.

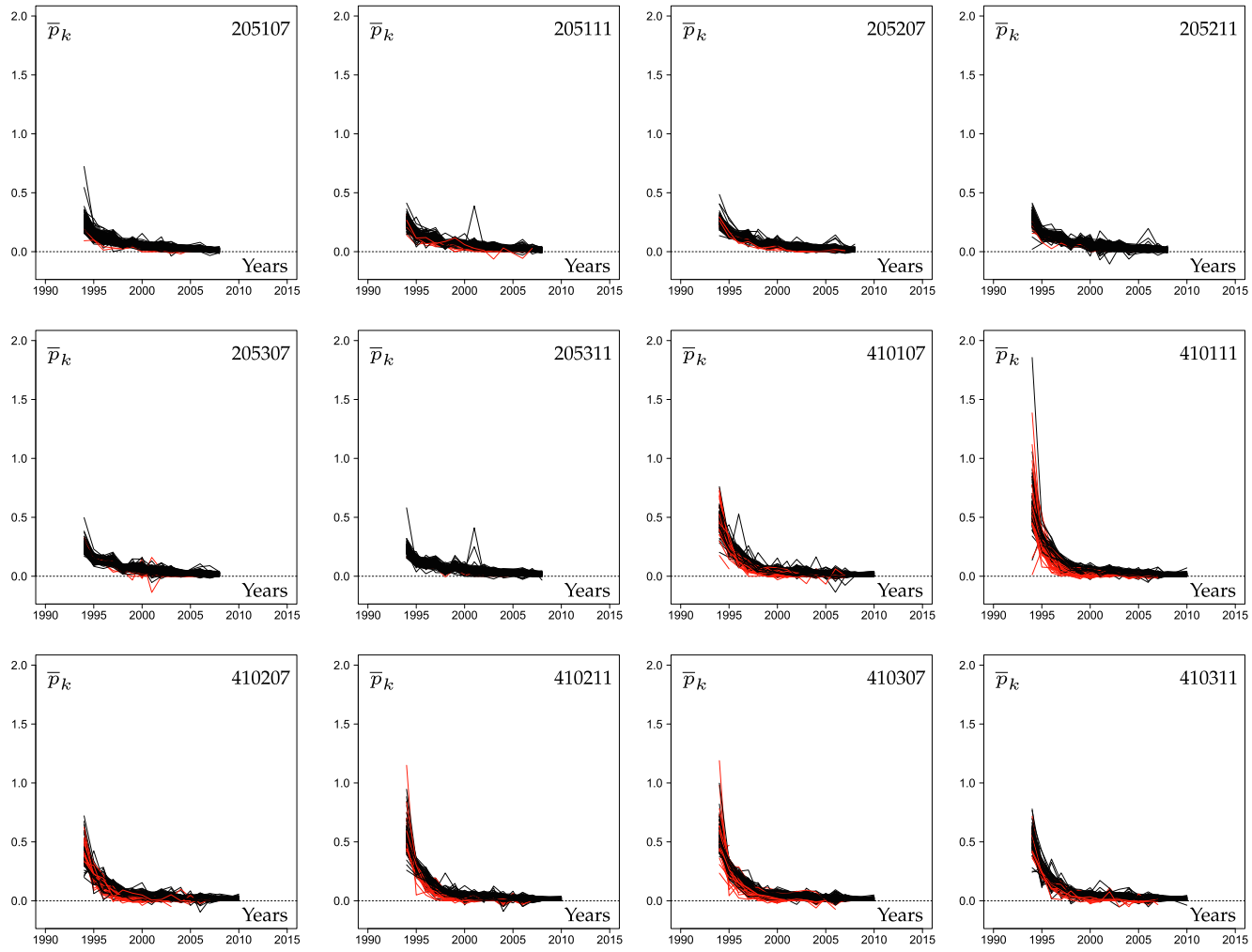

Fig. 3. The RGR ($\bar{p}_k$) trajectories of the individual trees of the *P. radiata* plots over the 14 (trial 205) and 16 (trial 410) survey years. Red colour highlights the trajectories of those trees that died before the end of the experiments. (For interpretation of the references to colour in this figure, the reader is referred to the web version of this article.)

Table 1
Synopsis of the plot and model specific parameters and statistical characteristics related to RGR and trial 205. SE – standard error of residuals, RMSE – root mean square error, Bias – bias. *B* and *E* are defined in Eqs. (9) and (10), respectively. The parameter symbols are explained in Section 2.1.

Model parameter	Plot number					
	205107	**205111**	**205207**	**205211**	**205307**	**205311**
c_1	0.15939	0.17217	0.16420	0.17574	0.17653	0.16720
c_2	55.98225	707.43522	334.12588	259.79045	602.37640	582.90519
a_0	0.06460	9.10519	4.07457	13.56038	8.17433	2.74637
a_1	1.03335	1.72485	1.70268	1.71785	1.64789	1.72615
b_0	0.68502	0.01503	0.03055	0.01192	0.01897	0.04251
b_1	−1.19737	0.17188	0.12805	0.21109	0.19763	0.11388
m_0	−5.34343	−6.11832	−5.10474	−5.73618	−7.40111	−6.30705
m_1	26.15888	29.99608	28.85575	20.82506	31.99057	27.69963
m_2	−60.12478	−38.95843	−76.58065	−32.74438	−15.18590	−38.91135
SE	0.03221	0.03101	0.02818	0.03779	0.03252	0.02767
RMSE	0.03218	0.03098	0.02816	0.03776	0.03250	0.02765
Bias	0.00244	−0.00001	−0.00001	0.00086	0.00072	−0.00024
B	0.03343	−0.00020	−0.00018	0.01096	0.00938	−0.00331
E	0.78160	0.77534	0.83856	0.72959	0.76758	0.79879

3.3. Model evaluation

The stem-diameter density distributions in the final survey year were all bell shaped as expected for data from tree plantations, i.e. the population size structure is comparatively simple (Fig. 4). All of these distributions were well reproduced by the model regardless of trial. A few minor shortcomings relate to the peaks of the density distributions, e.g. in plots 20511, 205207 and 205307. With plots 410111 and 410211, the observed curves were slightly outside the simulation envelopes for larger stem diameters.

Table 2
Synopsis of the plot and model specific parameters and statistical characteristics related to RGR and trial 410. SE – standard error of residuals, RMSE – root mean square error, Bias – bias. B and E are defined in Eqs. (9) and (10), respectively. The parameter symbols are explained in Section 2.1.

Model parameter	Plot number					
	410107	410111	410207	410211	410307	410311
c_1	0.13617	0.12535	0.13688	0.12665	0.12566	0.13014
c_2	226.30371	38.33011	82.24158	63.43836	46.88080	238.53881
a_0	0.04975	0.04580	0.04981	0.04422	0.04404	0.05010
a_1	1.33909	1.39201	1.39963	1.40244	1.38006	1.34378
b_0	0.40252	0.14389	0.62735	0.12559	0.05587	0.21272
b_1	−1.09374	−1.52683	−0.86982	−1.63586	−2.10826	−1.33389
m_0	−4.92848	−4.99777	−4.65150	−5.27744	−5.38258	−6.07952
m_1	40.27940	43.96823	30.88085	37.29797	42.48509	48.87110
m_2	−23.92730	−46.15290	−36.23400	−34.17041	−17.17859	−30.09111
SE	0.03712	0.04543	0.04543	0.03148	0.03404	0.03251
RMSE	0.03710	0.04540	0.04540	0.03146	0.03401	0.03249
Bias	0.00107	0.00084	−0.00086	0.00171	0.00138	0.00105
B	0.01155	0.00815	−0.01014	0.01792	0.01391	0.01132
E	0.91769	0.91925	0.84025	0.95029	0.94503	0.94051

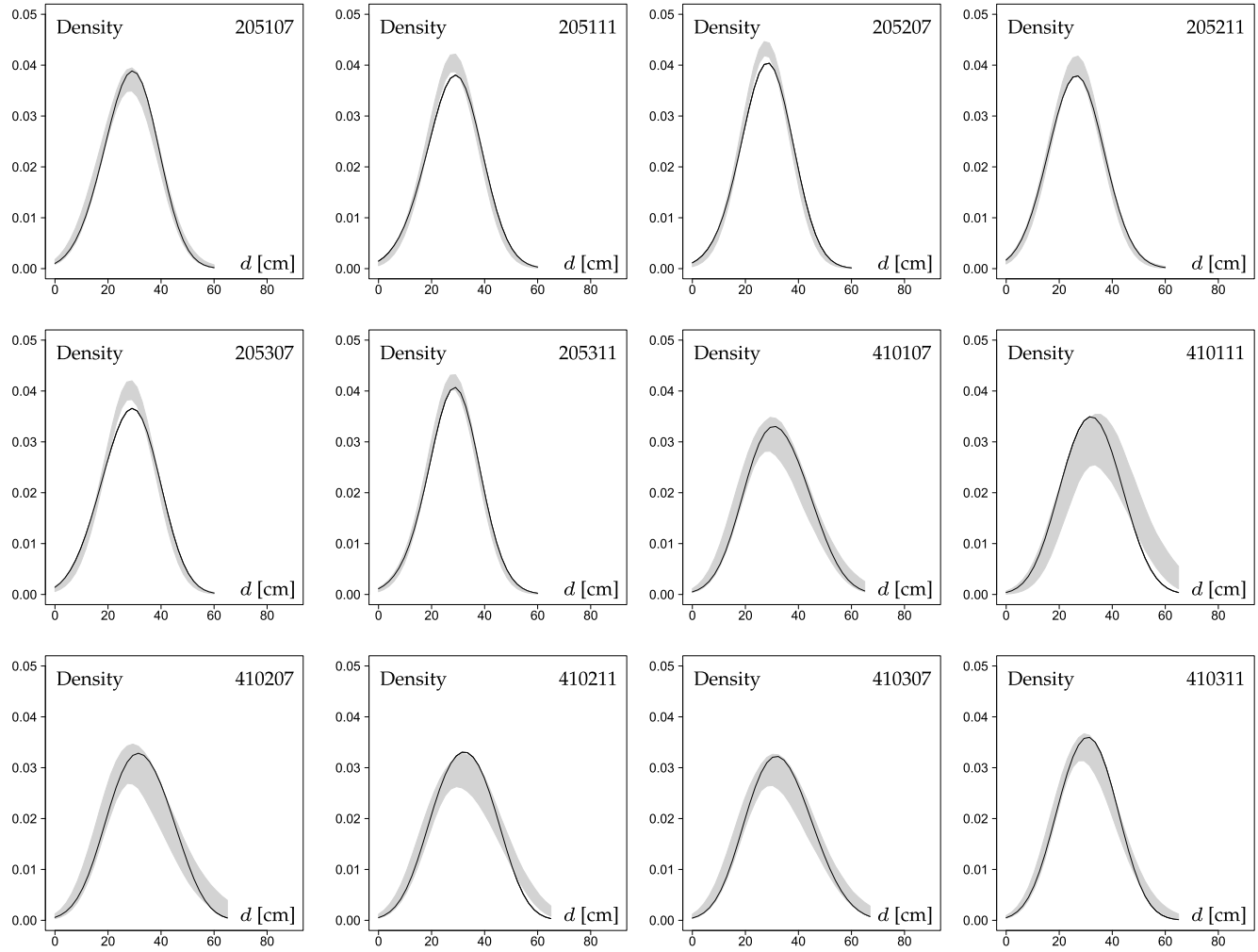

Fig. 4. Observed stem-diameter density distributions (continuous black line) of the 12 *P. radiata* plots in the final year of the experiments including the corresponding envelopes of 4499 model simulations using the global envelope test (Myllymäki et al., 2018). d is stem diameter.

Across all trials, the slope values of the relationship RGR-$d/\bar{d}$ first tended to increase and then to decrease in a non-linear fashion (Fig. 5). As such the slope of the linear RGR-$d/\bar{d}$ relationship followed a predictable pattern over mean population stem diameter (cf. Fig. 1). In early development stages, smaller trees have higher relative growth rates than larger trees. Over time the slope of the relationship increases and the larger trees in the corresponding data ellipses have a higher RGR than the smaller trees (Dyer, 1997). Stands with a stronger ontogenetic drift as in trial 410 consequently also tended to have much more varied slope curves than stands with a weaker ontogenetic drift (cf. Figs. 3 and 5). As this difference in ontogenetic drift between trials 205 and 410 was mainly caused by environmental conditions, the corresponding

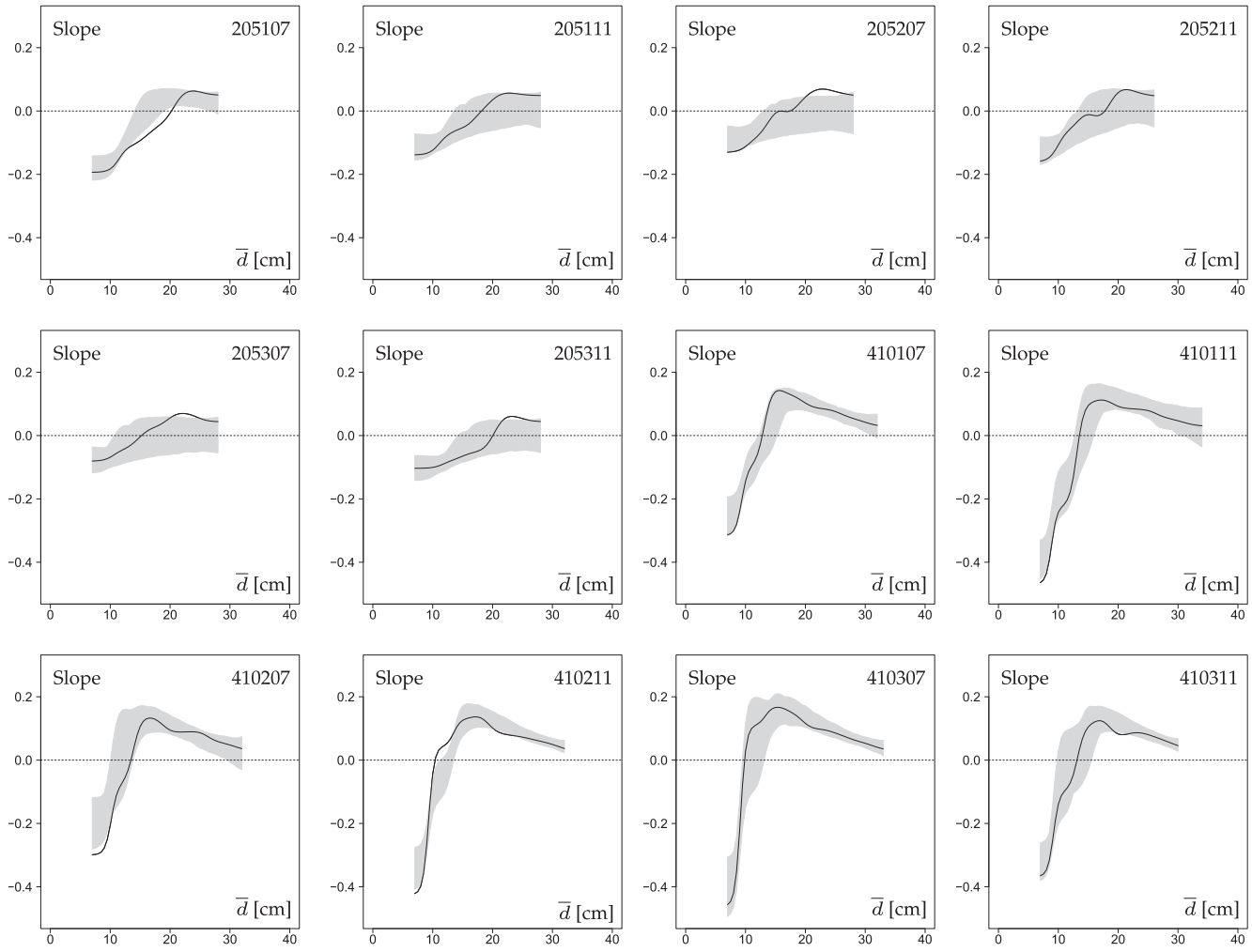

Fig. 5. Observed slopes f_1 (continuous black line) of the relationship RGR $= f_0 + f_1 \times d/\bar{d}$ in the 12 *P. radiata* plots including the corresponding envelopes of 4499 model simulations using the global envelope test (Myllymäki et al. 2018). $\bar{d}$ is mean stem diameter in different survey years.

differences in the slope curves reflect these conditions.

It is interesting that in trial 205 the peak of the slope curves commonly occurred after a population stem diameter $\bar{d} = 20$ cm whilst this peak generally forms before a mean diameter of 20 cm in trial 410 (Fig. 5). The same statement can be made for the $\bar{d}$ value where the sign of the slopes change from negative to positive. Thus, good environmental conditions clearly accelerate the temporal growth trend including the sequence of elliptic point clouds as described in Fig. 1. It is reasonable to expect the switch from negative to positive correlation between RGR and size to be associated with some critical point in stand development. Dyer (1997), Perry (1985) and Larocque and Marshall (1993) hypothesised this switch to mark the point when competition for resources begins to become more intense and to impact growth. It is remarkable how well the simulations have been able to reconstruct the complicated slope development. Minor issues where the observed slope curves were not fully within the envelopes can be seen in plots 205107, 205207, 205307, 410207 and 410211.

Compared to other studies (Binkley et al., 2006; Pommerening et al., 2016) the values of growth dominance G occurred in a limited range approximately between -0.15 and 0.25 and the relationship between the slope values of the relationship RGR-$d/\bar{d}$ and G was nonlinear (Fig. 6). The trend curves were similar to the solid black curves of observed slope values in Fig. 5. The reason for this is that G increased with increasing $\bar{d}$. At the beginning of stand development, all 12 plots surprisingly had negative G implying that small trees disproportionately contributed to basal-area growth and large trees did not dominate the growth of the plantation. This changed precisely when the slopes of the relationship RGR-$d/\bar{d}$ changed from negative to positive. At this point, G took a value of 0 in all 12 plots, i.e. here neither small nor large trees dominated the growth processes, but the growth of each tree was proportional to the size it contributes to overall population basal area. G further increased into the positive domain indicating that large trees increasingly dominated the plantation growth.

In all plots, maximum slope was located at values of G of approximately 0.1. Growth dominance, however, steadily kept increasing even after the slope maximum had been reached.

3.4. Parameter space

Mapping the standardised parameter space, as explained in Section 2.7, produced very varied results. Only in plot 410307 the standardised population parameters c_1 and c_2 were not far from the centre of the individual-tree parameter point cloud (Fig. 7). The peripheries of point clouds in plots 205107, 410111 and 410211 also included the population parameters. For all other plots the population parameters c_1 and c_2 were outside and at quite some distance from the individual-tree parameter point cloud. For all plots in trial 205 except for plot 205107 the c_2 parameters were so large that the much smaller individual-tree parameters $c_{i,t}^{(2)}$ formed the lower boundary of the parameter space at around -1, however, they varied slightly in value

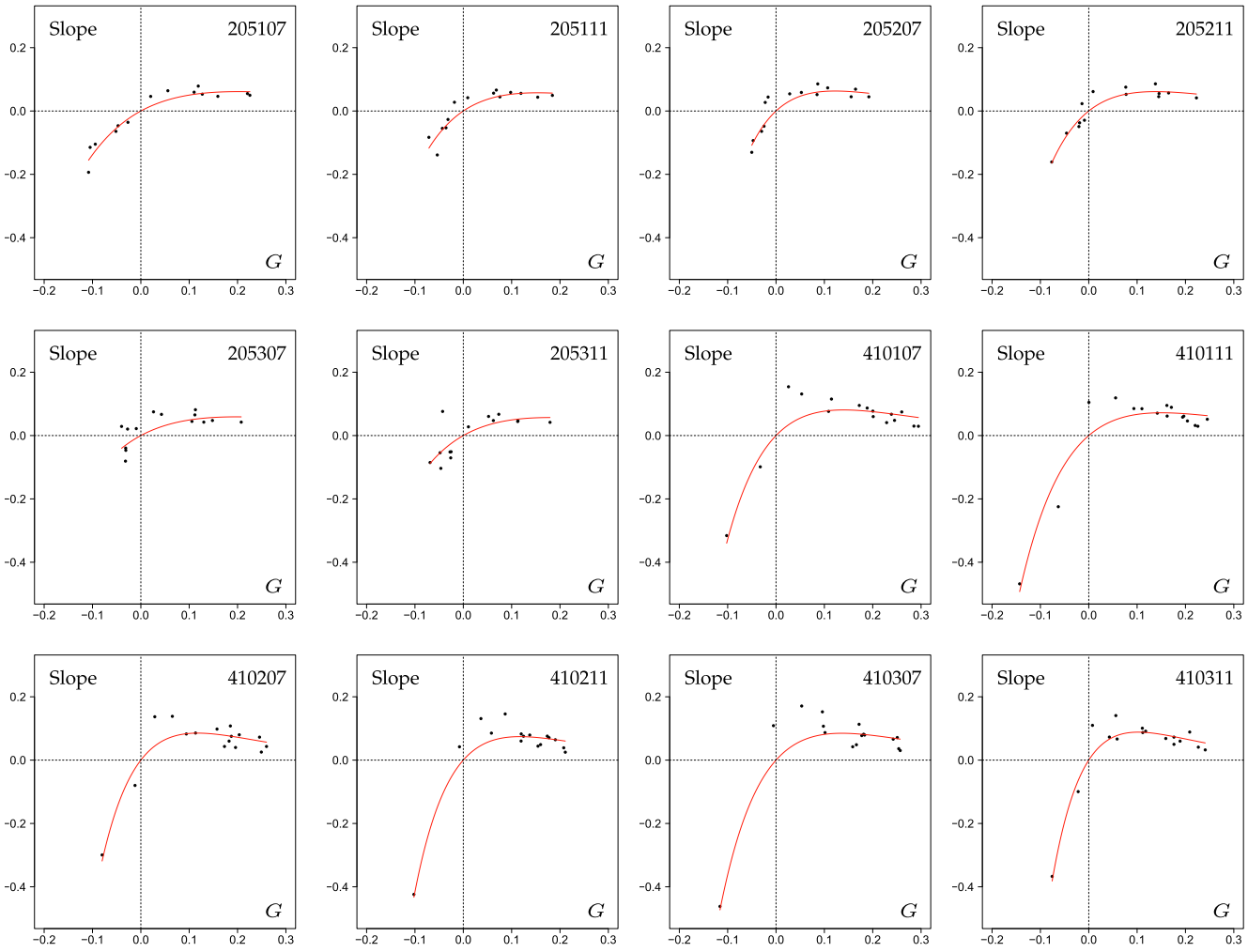

Fig. 6. Observed slopes f_1 of the relationship RGR $= f_0 + f_1 \times d/\bar{d}$ in the 12 *P. radiata* plots plotted over the growth dominance coefficient G (Binkley et al. 2006). G was calculated using individual-tree basal area $g = \pi(d/2)^2$ and the corresponding individual-tree mean annual absolute growth rates. The red trend curves were modelled using the Hassell function $f_1 = \frac{g_0 \times G}{(g_1+G)^{g_2}}$ (Bolker 2008), where g_0, g_1 and g_2 are model parameters. (For interpretation of the references to colour in this figure, the reader is referred to the web version of this article.)

within a very narrow range. It is interesting to note that for all these plots with standardised $c_{i,t}^{(2)}$ parameters around –1, model parameter b_1 was positive whilst for all other plots $b_1 < 0$. It seems reasonable to think that negative b_1 values substantially narrowed the range of $c_{i,t}^{(2)}$ parameters and reduced their magnitude. Small c_2 or $c_{i,t}^{(2)}$ values can lift RGR trajectories resulting in larger RGR values whilst very large values of the same parameters hardly make any difference to the trajectory locations. The individual-tree parameter point clouds in plots 410107, 410207 and 410311 were similar to those in the plots of trial 205 (except for that of 205107), only the range of $c_{i,t}^{(2)}$ values was larger and some $c_{i,t}^{(1)}$ values extended into the negative domain. With the notable exception of plot 410307, individual-tree parameters $c_{i,t}^{(2)}$ never much extended beyond 0, i.e. population c_2 was always substantially larger than any of the $c_{i,t}^{(2)}$.

For nearly all 12 plots with the exception of plot 410111 and perhaps plot 410211, individual-tree parameter $c_{i,t}^{(1)}$ was well spread across the horizontal parameter space with a clustering near 0, i.e. near the population c_1 value. Most $c_{i,t}^{(1)}$ lie between 0 and 1, i.e. in the majority of cases individual-tree and population parameters were similar in magnitude. In plots 205107, 410107, 410207, 410211, 410307 and 410311, i.e. in 6 out of 12 plots, negative standardised $c_{i,t}^{(1)}$ values occurred. Such values implied that the non-standardised values were slightly smaller than the c_1 population parameter. Small c_1 or $c_{i,t}^{(1)}$ values tend to push RGR trajectories upwards whilst large c_1 or $c_{i,t}^{(1)}$ values have the opposite effect. However, these effects are stronger than those caused by the c_2 or $c_{i,t}^{(2)}$ parameters, see Section 2.1. The extension of the $c_{i,t}^{(1)}$ point cloud into negative space was very limited and did not go beyond −0.1.

The temporal development showed that in most cases both $c_{i,t}^{(1)}$ and $c_{i,t}^{(2)}$ parameters were initially quite limited in range but then took much larger values as the years progressed. This effect increased the ontogenetic drift of RGR beyond the mean population trend which allowed the adaptation of the growth function in Eq. (2) to individual, observed RGR trajectories including temporary divergences.

4. Discussion and conclusions

The ontogenetic drift involved in RGR data and their dependence on size have triggered quite a few discussions in the past (Bragg, 2001; Rose et al., 2009; Rees et al., 2010). Arguments against RGR were partly

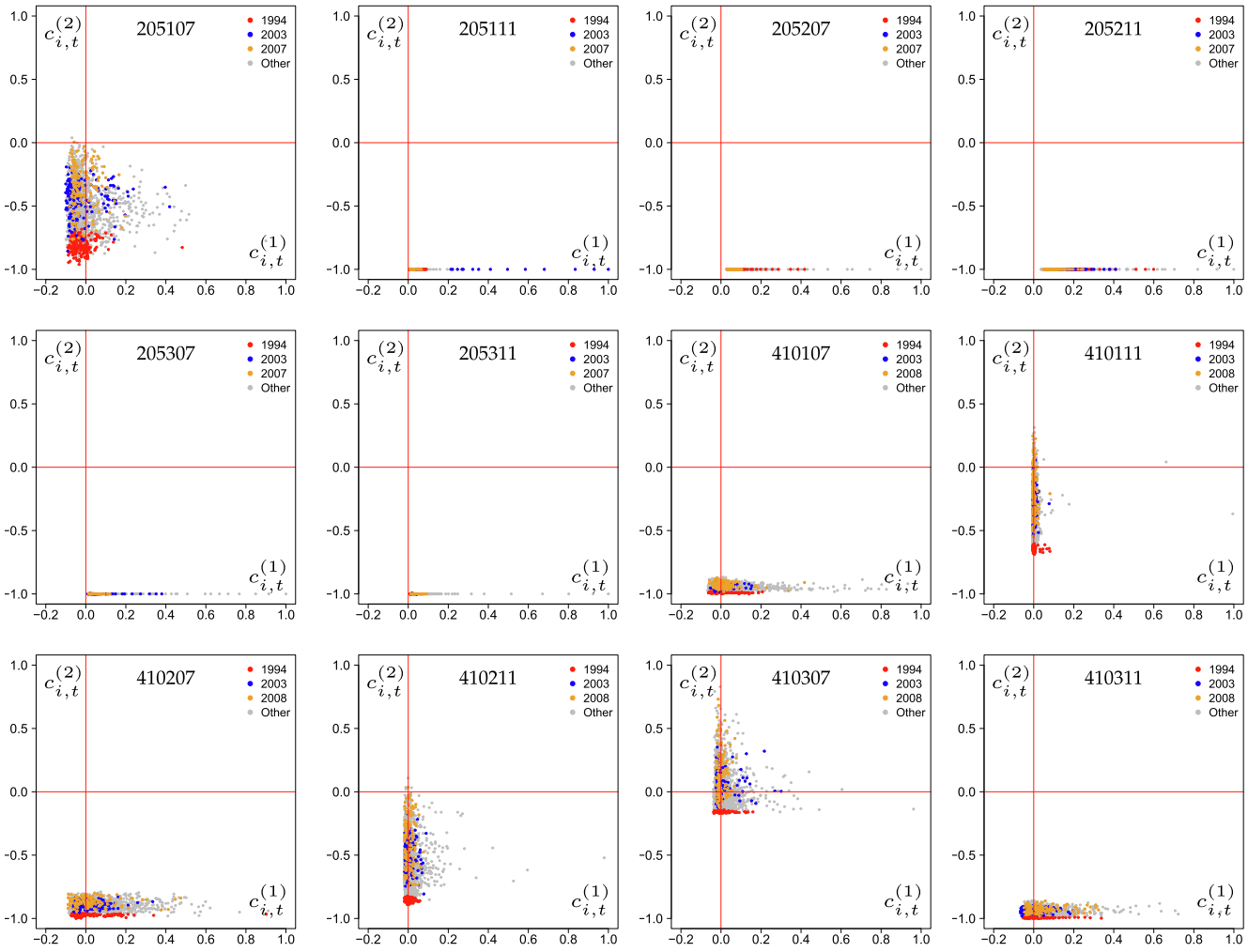

Fig. 7. Standardised individual-tree model parameters $c_{i,t}^{(1)}$ and $c_{i,t}^{(2)}$ in the context of population parameters c_1 and c_2 located at (0, 0).

related to the fact that growth in the experiments concerned were mostly considered as a summary and measured by an aggregated variable at the end of the experiment, e.g. total plant weight or total biomass measured after harvesting all plants. As these measurements usually are destructive, in most cases no time series with repeated measurements are available. Our research, however, has shown that the ontogenetic drift is one of many natural growth patterns of plants and according to our work the nature of its shape and course, i.e. velocity and steepness of curve, is related to environmental conditions and can be interpreted. Turnbull et al. (2008) more specifically argued that – because RGR typically decreases with size – classical growth analysis using RGR cannot distinguish between individuals that grow slowly because they are large and individuals that grow slowly because they are pursuing a slow growth strategy. They concluded that RGR alone therefore does not allow a fair comparison unless individuals are identically sized. However, our study revealed that by analysing repeated measurements, depicting RGR trajectories over size and reconstructing these trajectories through modelling it is indeed possible to distinguish these two situations.

Our research has demonstrated that RGR dynamics can be well described using a modelling approach originally developed by Wenk and colleagues (Wenk, 1994; Murphy and Pommerening, 2010) and the method provided a flexible approach towards explaining the mechanisms of the ontogenetic drift in plant populations. The original growth function used an age dependent variant of the Gompertz function (Gompertz, 1825) which we modified to become a size dependency (Eq. (2)). In our model, growth parameter c_1 has largely the same interpretation and a similar range of values as in the age-dependent model proposed by Wenk. We found that model parameter b_1 (Eq. (6)) clearly depends on the ontogenetic drift of RGR and through this drift on environmental conditions. Depending on the nature of the ontogenetic drift, b_1 can take positive or negative values. The evaluation characteristics highlighted that the model fit was better the stronger the ontogenetic drift. We could also show that trees with RGR trajectories located at or moving towards the bottom of the system of trajectories (Fig. 3) were likely to die and thus these results confirmed those of previous studies (Bigler and Bugmann, 2003; Gillner et al., 2013). Particularly the individual RGR trajectories of the mortality trees show that it is indeed possible to distinguish between different growth strategies.

Comparing population and individual-tree parameters yielded interesting and interpretable results. In most cases the population parameters were located outside the clouds of tree parameters which is related to the short-term adaptation behaviour of the growth function implemented in Eqs. (5) and (6). The aforementioned behaviour of parameter b_1 also substantially affected the relationship between c_2 and $c_{i,t}^{(2)}$. Negative b_1 pushed the individual-tree $c_{i,t}^{(2)}$ values towards the lower boundary of the parameter space and restricted them to a very narrow range. Parameter $c_{i,t}^{(1)}$ appeared to be less influenced by the sub-models in Eqs. (5) and (6) and covered quite well the whole parameter space with some clustering towards population parameter c_1. Only comparatively few $c_{i,t}^{(1)}$ values were smaller than c_1.

The slope values of the relationship RGR-$d/\bar{d}$ turned out to be a particularly useful characteristic for describing and explaining RGR dynamics including the ontogenetic drift. To date we have only seen it being used by Dyer (1997). The characteristic is directly related to the elliptic RGR-d data clouds and approximates the semi-major axes of the data ellipses through robust regression. The typical slope curve tends to start below 0 or near 0 and increases to reach a global maximum in the positive domain. Beyond that maximum, the slope curve gradually decreases again. The point on the size axis at which the slope changes from negative to positive, as well as the mean population size at which the maximum occurs, depends on the ontogenetic drift and thus on environmental conditions. Populations benefitting from benign environmental conditions show large negative initial slope values, a steep increase of the slope curve, and a peak at a comparatively small mean population size followed by a rapid decrease of slope value (cf. Fig. 5). With less beneficial conditions the slope curve starts with less negative values or even around 0, has a gradual increase towards a maximum at relatively large mean population sizes followed by a gradual decrease of slope value. Benign environmental conditions accelerate the temporal growth trend both in terms of reaching the slope maximum and abandoning it again in favour of smaller slope values. They also increase the ontogenetic drift and fertilisation would have a similar effect. Thinning interventions carried out as part of forest management in *Pinus taeda* L. plantations in Virginia (USA) have been shown to have the opposite effect, i.e. they reduced the magnitude of the slope (Dyer, 1997). The change from negative to positive slopes is clearly an important point in plant population development as Perry (1985), Larocque and Marshall (1993) and Dyer (1997) predicted. In Fig. 1, we can see that this change happens in plot 410211 sometime between 1994 and 1995, i.e. very early in stand development. Interestingly, the change from negative to positive slopes happens earlier on more productive sites than on less productive sites and at the point where growth dominance $G = 0$ (Fig. 6). Here small trees cease to dominate plantation growth and large trees start to take over the domination of growth in the population. At this point, size hierarchies have been largely sorted out.

Author contributions

All authors analysed the data, carried out the analyses and substantially contributed to the text. All persons entitled to co-authorships have been included in this paper. All authors have seen and approved the submitted version of the manuscript.

Declaration of Competing Interest

The authors declare that they have no known competing financial interests or personal relationships that could have appeared to influence the work reported in this paper.

Acknowledgements

Whilst this paper was in review, our co-author, mentor and friend Harold Burkhart passed away on 20 October 2022. Through his genuine kindness and extraordinary achievements Harold has been a constant source of inspiration to us. We wish to dedicate this paper to his living memory.

We thank Modelo Nacional de Simulación (MNS) and their current members for providing long-term growth series data of *P. radiata* trees including spatial tree locations required to carry out this study.

Availability of data and material

The data are available upon request from Modelo Nacional de Simulación (MNS) and enquiries should be directed to Guillermo Trincado on gtrincad@uach.cl. Sample R, C^{++} code and data relating to this study are available at https://zenodo.org/record/7341482 or using DOI https://doi.org/10.5281/zenodo.7341482.

Funding

This research did not receive any specific grant from funding agencies in the public, commercial or non-profit sectors.

References

Bigler, C., Bugmann, H., 2003. Growth-dependent tree mortality models based on tree rings. Can. J. For. Res. 33, 210–221.
Binkley, D., 2021. Forest Ecology. John Wiley & Sons, Chichester.
Binkley, D., Kashian, D.M., Boyden, S., Kaye, M.W., Bradford, J.B., Arthur, M.A., Fornwalt, P.J., Ryan, M.G., 2006. Patterns of growth dominance in forests of the Rocky Mountains, USA. Forest Ecol. Manage. 236, 193–201.
Blackman, V.H., 1919. The compound interest law and plant growth. Ann. Bot. 33, 353–360.
Bolker, B.M., 2008. Ecological models and data in R. Princeton University Press, Princeton.
Boyden, S., Binkley, D., Senock, R., 2005. Competition and facilitation between *Eucalyptus* and nitrogen-fixing *Falcataria* in relation to soil fertility. Ecology 86, 992–1001.
Bragg, D.C., 2001. Potential relative increment (PRI): a new method to empirically derive optimal tree diameter growth. Ecol. Model. 137, 77–92.
Burkhart, H.E., Tomé, M., 2012. Modeling forest trees and stands. Springer, New York.
Causton, D.R., 1977. A biologist's mathematics. Edward Arnold, London.
Clutter, J.L., Fortson, J.C., Pienaar, L.V., Brister, G.H., Bailey, R.L., 1983. Timber management. A quantitative approach. John Wiley & Sons, New York.
Dyer, M.E., 1997. Dominance/suppression competitive relationships in loblolly pine (*Pinus taeda* L.) plantations. PhD dissertation, Virginia Tech, Blacksburg, Virginia, USA.
Evans, G.C., 1972. The quantitative analysis of plant growth. Blackwell Scientific Publications, Oxford.
Fisher, R.A., 1921. Some remarks on the methods formulated in a recent article on "The quantitative analysis of plant growth". Ann. Appl. Biol. 7, 367–372.
Freckleton, R.P., Watkinson, A.R., 2001. Asymmetric competition between plant species. Funct. Ecol. 15, 615–623.
Gillner, S., Rüger, N., Roloff, A., Berger, U., 2013. Low relative growth rates predict future mortality of common beech *Fagus sylvatica* L.). For. Ecol. Manage. 2013, 372–378.
Gompertz, B., 1825. On the nature of the function expressive of the law of human mortality, and on a new mode of determining the value of life contingencies. Philos. Trans. R. Soc. 115, 513–585.
Grime, J.P., 1977. Evidence for the existence of three primary strategies in plants and its relevance to ecological and evolutionary theory. Am. Nat. 111, 1169–1194.
Houghton, J., Thompson, K., Rees, M., 2013. Does seed mass drive the differences in relative growth rate between growth forms? Proc. R. Soc. B 280, 20130921.
Hunt, R., 1982. Plant growth curves. The functional approach to plant growth analysis. Cambridge University Press, Cambridge.
Hunt, R., 1990. Basic growth analysis: Plant growth analysis for beginners. Unwin Hyman, London.
Iida, Y., Poorter, L., Sterck, F., Rahman Kassim, A., Potts, M.D., Kubo, T., Kohyama, T.S., 2014. Linking size-dependent growth and mortality with architectural traits across 145 co-occuring tropical tree species. Ecology 95, 353–363.
Illian, J., Penttinen, A., Stoyan, H., Stoyan, D., 2008. Statistical analysis and modelling of spatial point patterns. John Wiley & Sons, Chichester.
Larocque, G.R., Marshall, P.L., 1993. Evaluating the impact of competition using relative growth rate in red pine (*Pinus resinosa* Ait.) stands. For. Ecol. Manage. 58, 65–83.
Lorenz, M.O., 1905. Methods for measuring the concentration of wealth. American Statistics Association 9, 209–219.
Murphy, S.T., Pommerening, A., 2010. Modelling the growth of Sitka spruce (*Picea sitchensis* (Bong.) Carr.) in Wales using Wenk's model approach. Allgemeine Forst- und Jagdzeitung 181, 35–43.
Myllymäki, M., Mrkvička, T., 2019. GET: Global envelopes in R. arXiv:1911.06583 [stat. ME].
Myllymäki, M., Mrkvička, T., Grabarnik, P., Seijo, H., Hahn, U., 2018. Global envelope tests for spatial processes. J. R. Stat. Soc. Ser. B 79, 381–404.
Niklas, K.J., 1994. Plant allometry: The scaling of form and process. University of Chicago Press, Chicago.
Perry, D.A., 1985. The competition process in forest stands. In: Cannell, M.G.R., Jackson, J.E. (Eds.), Attributes of Trees as Crop Plants. Institute of Terrestrial Ecolohy, Abbots Ripton, Hunts, pp. 481–506.
Pommerening, A., Muszta, A., 2016. Relative plant growth revisited: Towards a mathematical standardisation of separate approaches. Ecol. Model. 320, 383–392.
Pommerening, A., Brzeziecki, B., Binkley, D., 2016. Are long-term changes in plant species composition related to asymmetric growth dominance in the pristine Białowieża Forest? Basic Appl. Ecol. 17, 408–417.
Pommerening, A., Grabarnik, P., 2019. Individual-based methods of forest ecology and management. Springer, Cham.
Pommerening, A., Szmyt, J., Zhang, G., 2020. A new nearest-neighbour index for monitoring spatial size diversity: The hyperbolic tangent index. Ecol. Model. 435, 109232.

R Development Core Team, 2021. R: A language and environment for statistical computing. R Foundation for Statistical Computing, Vienna, Austria http://www.r-project.org.
Ramseier, J., Weiner, A., 2006. Competitive effect is a linear function of neighbour biomass in experimental populations of *Kochia scoparia*. J. Ecol. 94, 305–309.
Rees, M., Osborne, C.P., Woodward, F.I., Hulme, S.P., Turnbull, L.A., Taylor, S.H., 2010. Partitioning the components of relative growth rate: How important is plant size variation. Am. Nat. 176, E152–E161.
Rose, K.E., Atkinson, R.L., Turnbull, L.A., Rees, M., 2009. The costs and benefits of fast living. Ecol. Lett. 12, 1379–1384.
Ryan, M.G., Phillips, N., Bond, B.J., 2006. The hydraulic limitation hypothesis revisited. Plant Cell Environ. 29, 367–381.
Ryan, M.G., Yoder, B.J., 1997. Hydraulic limits to tree height and tree growth. Bioscience 47, 235–242.
Salas-Eljatib, C., Weiskittel, A.R., 2020. On studying the patterns of individual-tree mortality in natural forests: A modelling analysis. For. Ecol. Manage. 475, 118369.
Turnbull, L.A., Paul-Victor, C., Schmid, B., Purves, D.W., 2008. Growth rates, seed size, and physiology: Do small-seeded species really grow faster? Ecology 89, 1352–1363.
Weiner, J., Stoll, P., Muller-Landau, H., Jasentuliyana, A., 2001. The effects of density, spatial pattern, and competitive symmetry on size variation in simulated plant populations. Am. Nat. 158, 438–450.
Weiskittel, A.R., Hann, D.W., Kerschaw, J.A., Vanclay, J.K., 2011. Forest growth and yield modeling. Wiley Blackwell, Chichester, p. 415p.
Wenk, G., 1969. Eine neue Wachstumsgleichung und ihr praktischer Nutzen zur Herleitung von Volumenzuwachsprozenten. [A new growth equation and its practical use to derive volume increment.]. Archiv für Forstwesen 18, 1085–1094.
Wenk, G., 1994. A yield prediction model for pure and mixed stands. For. Ecol. Manage. 69, 259–268.
Wenk, G., Antanaitis, V., Šmelko, Š., 1990. Waldertragslehre. [Forest growth and yield science.] Deutscher Landwirtschaftsverlag. Berlin.
West, P.W., 2014. Calculation of the growth dominance statistic for forest stands. For. Sci. 60, 1021–1023.
West, P.W., 2020. Do increasing respiratory costs explain the decline with age of forest growth rate? J. For. Res. 31, 693–712.
Whitehead, F.H., Myerscough, P.J., 1962. Growth analysis of plants. The ratio of mean relative growth rate to mean relative rate of leaf area increase. New Phytol. 61, 314–321.
Yoda, K., Shinozaki, K., Ogawa, H., Hozumi, K., Kira, T., 1965. Estimation of the total amount of respiration in woody organs of trees and forest communities. Journal of Biology, Osaka City University 15, 15–26.